Analysis of influent parameters during infrared radiative heating of PET preform

Fabrice Schmidt, Serge Monteix, Yannick Le Maoult, Gérard Denis

To cite this version:

Fabrice Schmidt, Serge Monteix, Yannick Le Maoult, Gérard Denis. Analysis of influent parameters during infrared radiative heating of PET preform. International Conference of Polymer Processing Society, Jun 2000, Shangaï, China. hal-02056287

HAL Id: hal-02056287
https://hal-mines-albi.archives-ouvertes.fr/hal-02056287
Submitted on 14 Mar 2019

ANALYSIS OF INFLUENT PARAMETERS DURING INFRARED RADIATIVE HEATING OF PET PREFORM

S. Monteix (1), F.M. Schmidt (1)*, Y. Le Maoult (1) and G. Denis (2)

(1) ECOLE DES MINES d'Albi-Carmaux, Campus Jarlard, Route de Teillet,
81013 ALBI CT Cedex 09 (FRANCE)
(2) PERRIER-VITTEL M.T. B.P. 43, 88805 VITTEL Cedex (FRANCE)

The processing parameters during radiative heating of PET preform are:

- The number of infrared heaters N_h,
- The temperature T_i of each infrared heater $L_{i=1,N_h}$
- The heating time t_h,
- The cooling time t_c,
- The coordinate vector $\vec{x}_{i=1,N_h}$ of each infrared heater $L_{i=1,N_h}$,
- The heat transfer coefficient h_c between cooling air and PET preform.

In previous papers [1,2], the spectral emissivity and directivity of different halogen lamps (Philips 300-700W electric nominal power made of a coiled tungsten filament, contained in a quartz tubular enclosure and a diffuse reflector made of a ceramic coating) have been reported. Recent measurements using a 0.6-25 μm thermopile sensor on similar halogen lamps of 1000W (used in an industrial oven of injection-blow moulding machine) have been processed. The maximum temperature of the tungsten filament is 2400 K. As shown in fig. 1, these infrared heaters exhibit a slightly different behaviour from a lambertian source (diffuse radiation) due to the reflector. The average discrepancy is about 8 %. In order to take into account the participation of the diffuse reflector in the amount of the incident radiation, a coefficient of efficacy k_{rf} is introduced.

Fig. 2 shows the experimental set-up that has been developed in order to measure the surface temperature distribution (front face and back face), when a PET sheet is heating using previous infrared heaters. An 880 LW AGEMA infrared camera (8-12 μm bandwidth) is used to measure the spatial and transient temperature distribution. The surface dimension of the PET sheet is $20\text{cm} \times 20\text{cm}$ cm and the thickness is 1.5 mm.

A 3D control-volume model has been developed for computing radiative heat transfer during the infrared heating stage. The sheet-shape domain sketched in fig. 3 is discretised into cubic elements, called control-volumes [3]. The energy equation including radiative transfer integrated over each control volume $V_e = \Delta x \Delta y \Delta z$ and over the time from t to $t + \Delta t$ leads to:

---

[*] Corresponding author

$$\int_{\Delta t}\int_{\Omega_e}\rho c_p \frac{\partial T}{\partial t}\, d\Omega\, dt = \int_{\Delta t}\int_{\Gamma_e} k\left(\vec{\nabla} T.\vec{n}\right) d\Gamma\, dt + \int_{\Delta t}\int_{\Gamma_e} \vec{\varphi}_r.\vec{n}\, d\Gamma\, dt \qquad (1)$$

Where ρ is the specific mass, c_p the heat capacity, k the heat conductivity. Γ_e is the surface of control-volume V_e. The assumption of “cold material” is convenient, as the PET bulk temperature $(\cong 120°C)$ is very low in comparison to heaters temperature $(1500-2000°C)$. Consequently, the net radiative transfer over each control yields:

$$\int_{\Gamma_e} \vec{\varphi}_r.\vec{n}\, d\Gamma = k_{rf}\, F \frac{\Gamma_i}{\Gamma_e} \int_{\Delta\lambda} \varepsilon_\lambda (T_i)\, \pi L_\lambda^0 (T_i) \left(\tau_\lambda^{\frac{y_1}{e}} - \tau_\lambda^{\frac{y_2}{e}} \right) d\lambda \qquad (2)$$

Where e is the thickness of the PET film used to obtain an intrinsic transmission coefficient τ_λ, ε_λ is the spectral tungsten emissivity, L_λ^0 is the black body intensity. The diffuse view factor F is computed using the contour integration method [4].

The integration of equation (1) over all the control-volumes leads to a set of linear algebraic equations, which is solved iteratively using the line by line Gauss-Seidel method in the y-direction to obtain a 3D-system computed by the TDMA algorithm.

An example of PET sheet heating has been processed. The dimensions of the sheet as well as the halogen lamps are sketched in fig.4. The thickness of the sheet is 3mm. The processing parameters for the infrared heaters are summarised in the table below. It is to be noted that in this simplified case, the distance between the lamps and the front face of the sheet is constant and equals to 50mm.

	T_i (K)	x_i (mm)	y_i (mm)	z_i (mm)
$L_{i=1}$	2200	40	-50	20
$L_{i=2}$	2000	40	-50	40
$L_{i=3}$	1700	40	-50	60
$L_{i=4}$	2000	40	-50	80
$L_{i=5}$	2200	40	-50	100

The heating time t_h is 35 s and the cooling time t_c is 25s. A constant heat transfer coefficient of 10 $W m^{-2} K^{-1}$ is applied to the back and front faces of the sheet. The temperature distribution of the front face of the sheet is plotted as shown in fig. 5. In addition, fig. 6 shows the temperature distribution throughout the thickness versus time. The temperatures of the central lamps $L_{i=2,3,4}$ have been decreased in order to improve the temperature distribution on the front face.

Simulations results will be further discussed during the podium presentation.

REFERENCES

[1] Monteix S., F. Schmidt, Le Maoult Y., R. Ben Yedder, R. DiRaddo, D. Laroche, « Experimental Study and Numerical Simulation of Preform or Sheet Infrared Radiative Heating », in Proceeding of AMPT '99, Dublin (Ireland), 3-6 August, 1999

[2] Monteix S., R. DiRaddo, F. Schmidt, Le Maoult Y. «Profiled infrared radiative heating in blow moulding and thermoforming» PPS'98 - North American Meeting, Toronto, Canada, Aug 17- 19, pp. 147-148, 1998

[3] S.V. Patankar, "Numerical Heat Transfer and Fluid Flow", Ed. Mc Graw Hill, New-York (1980)

[4] R. Rammohan, "Efficient Evaluation of Diffuse View Factors for Radiation", Int. J. Heat Mass Transfer 39(1996) 1281-1286

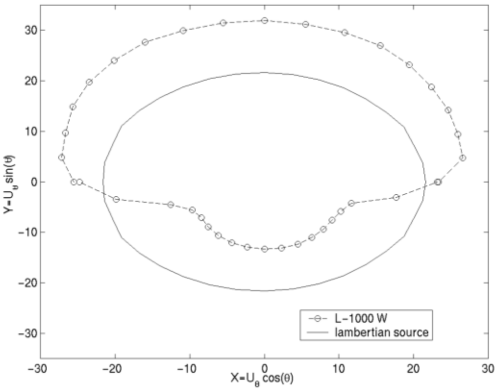

Figure 1: Halogen lamps (1000 W) directivity

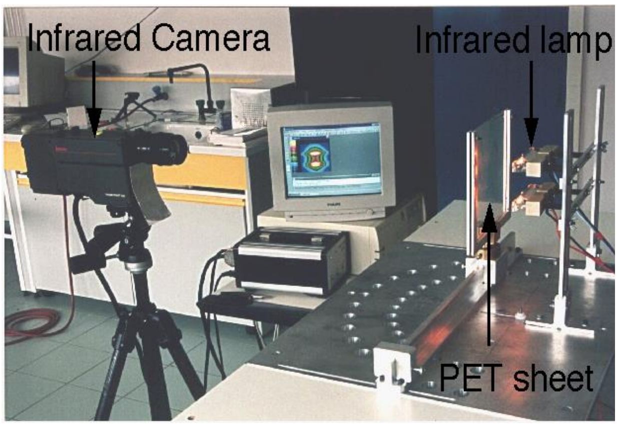

Figure 2: Experimental set-up for surface temperature distribution

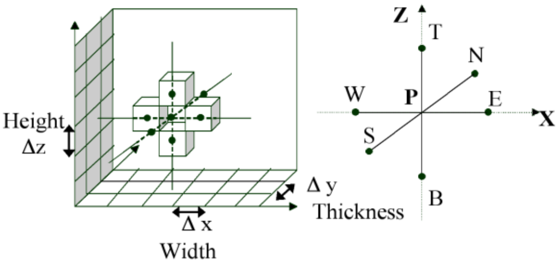

Figure 3: 3Dcontrol-volumes

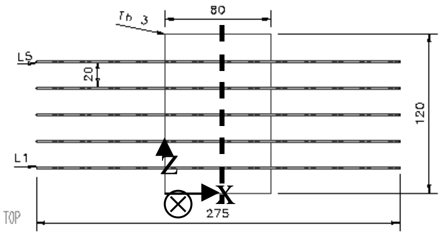

Fig.4: Dimensions of the sheet and the halogen lamps

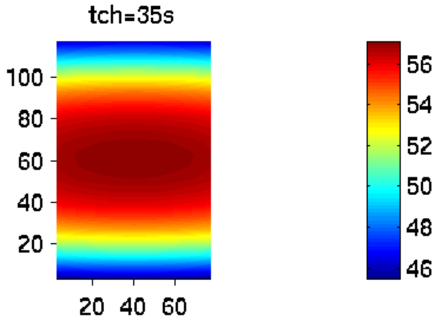

Fig. 5: Temperature distribution on the front face $(t_h = 35s)$

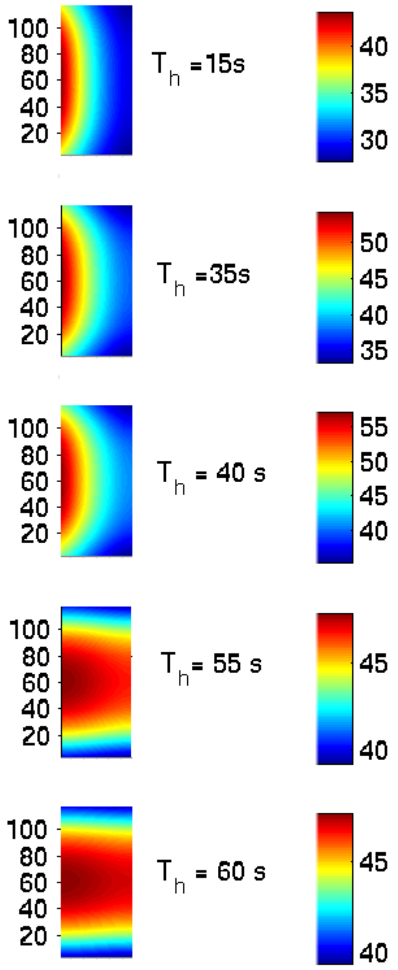

Fig. 6: Temperature distribution throughout the thickness versus time